Cell PRESS
Open ACCESS

Cell Reports
Article

Pleiotrophin Regulates the Retention and Self-Renewal of Hematopoietic Stem Cells in the Bone Marrow Vascular Niche

Heather A. Himburg,[1] Jeffrey R. Harris,[1] Takahiro Ito,[4] Pamela Daher,[1] J. Lauren Russell,[1] Mamle Quarmyne,[1] Phuong L. Doan,[1] Katherine Helms,[1] Mai Nakamura,[1] Emma Fixsen,[1] Gonzalo Herradon,[5] Tannishtha Reya,[4] Nelson J. Chao,[1,2] Sheila Harroch,[6] and John P. Chute[1,3,*]

[1]Division of Cellular Therapy, Department of Medicine, Duke University Medical Center
[2]Department of Immunology
[3]Department of Pharmacology and Cancer Biology
Duke University, Durham, NC 27710, USA
[4]Department of Pharmacology, University of San Diego, San Diego, CA 92093, USA
[5]Pharmacology Laboratory, Department of Pharmaceutical and Food Sciences, Facultad de Farmacia, Universidad CEU San Pablo, 28003 Madrid, Spain
[6]Department of Neuroscience, Pasteur Institute, 75724 Paris, France
*Correspondence: john.chute@duke.edu
http://dx.doi.org/10.1016/j.celrep.2012.09.002

SUMMARY

The mechanisms through which the bone marrow (BM) microenvironment regulates hematopoietic stem cell (HSC) fate remain incompletely understood. We examined the role of the heparin-binding growth factor pleiotrophin (PTN) in regulating HSC function in the niche. PTN$^{-/-}$ mice displayed significantly decreased BM HSC content and impaired hematopoietic regeneration following myelosuppression. Conversely, mice lacking protein tyrosine phosphatase receptor zeta, which is inactivated by PTN, displayed significantly increased BM HSC content. Transplant studies revealed that PTN action was not HSC autonomous, but rather was mediated by the BM microenvironment. Interestingly, PTN was differentially expressed and secreted by BM sinusoidal endothelial cells within the vascular niche. Furthermore, systemic administration of anti-PTN antibody in mice substantially impaired both the homing of hematopoietic progenitor cells to the niche and the retention of BM HSCs in the niche. PTN is a secreted component of the BM vascular niche that regulates HSC self-renewal and retention in vivo.

INTRODUCTION

Hematopoietic stem cells (HSCs) are capable of self-renewal and reconstitution of the entire blood and immune system in vivo. HSC fate determination in vivo is regulated by a combination of intrinsic mechanisms and environmental cues mediated via cell-cell interactions, cytokines, and secreted growth factors (Blank et al., 2008; Kiel and Morrison, 2008; Zon, 2008) Although characterization of the cells within the bone marrow (BM) microenvironment that regulate HSC fate continues to evolve (Butler et al., 2010; Calvi et al., 2003; Ding et al., 2012; Hooper et al., 2009; Kiel et al., 2005; Méndez-Ferrer et al., 2010; Salter et al., 2009; Zhang et al., 2003), the mechanisms through which BM-microenvironment cells regulate HSC functions are less well understood.

We previously showed that adult sources of endothelial cells (ECs) were capable of supporting the expansion of murine and human HSCs in vitro (Chute et al., 2002, 2004, 2005, 2006a). Utilizing a genomic screen of primary adult human brain ECs (HUBECs) that support HSC expansion in noncontact cultures (Chute et al., 2002, 2005, 2006a), we identified pleiotrophin (PTN,) a heparin-binding growth factor that is primarily expressed in the nervous system (Li et al., 1990), to be >100-fold overexpressed in HUBECs compared with non-HSC-supportive ECs (Himburg et al., 2010). We subsequently showed that in vitro treatment of murine BM HSCs with PTN, in combination with other cytokines, supported the expansion of HSCs with long-term (LT) repopulating capacity (Himburg et al., 2010). However, it remained unknown whether PTN was expressed by cells within the HSC niche, which regulates HSC function in vivo, or whether PTN had any physiologically relevant function in regulating HSC fate in vivo. We therefore sought to determine whether PTN is expressed by BM-microenvironment cells within the HSC niche, and whether modulation of PTN expression within the niche can affect the maintenance, regeneration, or retention of HSCs in vivo. Here, we show that PTN is uniquely expressed and secreted by BM sinusoidal ECs within the HSC vascular niche and has an important role in regulating HSC self-renewal and retention in the BM.

RESULTS

PTN Regulates HSC Self-Renewal and Is Necessary for Hematopoietic Regeneration In Vivo

We first examined the hematologic phenotype of mice bearing a constitutive deletion of *ptn* (PTN$^{-/-}$ mice) compared with littermate control PTN$^{+/+}$ mice. Knockout of *ptn* in the mouse strain was confirmed by RT-PCR analysis (Figure 1A). Eight-week-old

PTN$^{-/-}$ mice displayed no significant differences in peripheral blood (PB) complete blood counts or spleen size (Figure S1). We also observed no differences in BM vascular density between PTN$^{-/-}$ mice and PTN$^{+/+}$ mice (data not shown). However, adult PTN $^{-/-}$ mice contained significantly decreased BM c-kit^{+}sca-1^{+}lineage^{-} (KSL) stem/progenitor cells as well as BM colony-forming unit (CFU) spleen day 12 cells (CFU-S12; Figure 1B). Furthermore, the PTN$^{-/-}$ mice contained significantly decreased numbers of BM SLAM-receptor (CD150^{+}CD48^{-} CD41^{-})-positive KSL (SLAM^{+}KSL) cells (Kiel et al., 2005) compared with PTN$^{+/+}$ mice, reflecting a deficit in phenotypic HSCs (Figure 1B). Importantly, competitive transplantation assays of BM 34^{-}KSL cells, which are highly enriched for HSCs (Himburg et al., 2010), into lethally irradiated congenic mice confirmed a marked decrease in LT-HSC content in PTN$^{-/-}$ mice compared with PTN $^{+/+}$ mice. At 12 weeks after competitive transplantation, donor CD45.2^{+} PB cell engraftment was 7-fold lower in mice that were transplanted with BM 34^{-}KSL cells from PTN$^{-/-}$ mice compared with recipients of BM 34^{-}KSL cells from PTN$^{+/+}$ mice (mean 5% versus 35%; Figure 1C). Multilineage engraftment of myeloid cells, erythroid cells, B cells, and T cells was also significantly lower in mice transplanted with BM HSCs from PTN$^{-/-}$ mice compared with recipients transplanted with BM HSCs from PTN$^{+/+}$ mice (Figure 1D). Analysis over time revealed that mice transplanted with BM HSCs from PTN$^{-/-}$ mice had 5- to 20-fold decreased donor cell repopulation between 4 weeks and 20 weeks posttransplant compared with mice transplanted with HSCs from PTN$^{+/+}$ mice, confirming a loss of both short-term (ST) and LT HSCs in PTN$^{-/-}$ mice (Figure 1C). Poisson statistical analysis of a limiting dilution transplant assay demonstrated that the competitive repopulating unit (CRU) frequency within PTN $^{-/-}$ mice was 11-fold decreased (1 in 66 cells; 95% confidence interval (CI): 1/37–1/119) compared with the CRU frequency in PTN $^{+/+}$ mice (1 in 6; CI: 1/2–1/14; Figure 1E). Taken together, these results demonstrate that PTN regulates the maintenance of the BM HSC pool.

Because deletion of PTN caused a substantial reduction in BM HSC content in vivo, we next sought to determine whether PTN deletion affected hematopoietic regeneration following myelosuppressive injury. We irradiated adult PTN$^{-/-}$ mice and PTN$^{+/+}$ mice with 700 cGy total body irradiation (TBI), a myelosuppressive radiation dose, and compared their survival through day +30. Sixty-nine percent of the PTN$^{+/+}$ mice (11 of 16) remained alive and well through day +30 (Figure 1F). In contrast, none of the PTN$^{-/-}$ mice (0 of 7) survived past day +18 post-TBI, indicating markedly increased radiosensitivity in PTN$^{-/-}$ mice. Commensurate with this, PTN$^{-/-}$ mice displayed severely decreased BM progenitor cell content at day +20, whereas PTN $^{+/+}$ mice showed evidence of recovery of the BM progenitor cell compartment (Figure 1G). Taken together, these results demonstrate that PTN is essential for hematopoietic regeneration and survival following radiation-induced myelosuppression.

PTN Regulates the HSC Pool in a Microenvironment-Dependent Manner

To determine whether PTN signaling is HSC autonomous or dependent on the BM microenvironment, we transplanted BM cells from CD45.1^{+} Bl6.SJL mice into lethally irradiated PTN$^{-/-}$ mice or PTN$^{+/+}$ mice (CD45.2^{+}) and compared the hematopoietic phenotypes of these chimeric mice. At 8 weeks posttransplant, recipient mice demonstrated >95% donor chimerism (mean 96.4% donor cells in wild-type [WT];PTN$^{+/+}$ mice and 95.2% in WT;PTN$^{-/-}$ mice, n = 8–9 mice/group). Adult PTN$^{-/-}$ mice that were transplanted with BM cells from Bl6.SJL mice (WT;PTN$^{-/-}$ mice) displayed significantly decreased numbers of BM KSL cells, CFU-S12, and SLAM^{+}KSL HSCs compared with age-matched WT;PTN$^{+/+}$ mice (Figure 1H). Importantly, mice that were competitively transplanted with BM from WT;PTN$^{-/-}$ mice also displayed significantly decreased multilineage donor cell repopulation between 4 weeks and 30 weeks posttransplant compared with mice transplanted with the identical dose of BM cells from WT;PTN$^{+/+}$ mice (Figure 1I). Secondary transplantation of BM cells from the primary transplant recipients demonstrated that secondary mice in the WT;PTN$^{-/-}$ group had 4-fold decreased donor cell engraftment at 8 weeks posttransplant compared with secondary recipients in the WT;PTN$^{+/+}$ group (mean donor CD45.1^{+} cells: 0.5% ± 0.2 versus 2.0% ± 0.7, p = 0.04, n = 8–9/group). These results demonstrate that PTN production by the BM microenvironment is necessary for regeneration of the HSC pool following BM transplantation.

Because PTN was necessary for normal HSC reconstitution in vivo following BM transplantation, we next tested whether pharmacologic administration of PTN could accelerate HSC reconstitution in a clinically relevant model of HSC transplantation. We transplanted limiting doses (0.5–1 × 10^{6} cells) of human cord blood (CB) mononuclear cells intravenously into NOD/SCID IL2R-$\gamma^{-/-}$ (NSG) mice, and compared human hematopoietic reconstitution over time in mice that were treated intraperitoneally with 2–4 μg PTN or saline on days +7, +10, and +13 posttransplant. PB was analyzed at 4 and 8 weeks posttransplant for human CD45^{+} cell engraftment. The PTN-treated mice demonstrated significantly increased human CD45^{+} cell repopulation compared with saline-treated mice over time (4 weeks: mean 10.9% huCD45^{+} versus 1.4%; 8 weeks: mean 9.9% versus 1.9%, n = 11–14 mice/group; Figure 1J). Importantly, NSG mice that were treated with PTN also had a >10-fold increased human hematopoietic progenitor cell (HPC) content in the BM at 8 weeks posttransplant compared with saline-treated controls (Figure 1J). These results show that PTN promotes human hematopoietic stem/progenitor cell (HSPC) regeneration in vivo following transplantation, and illustrate the translational potential of PTN administration as a means to accelerate human hematopoietic reconstitution, particularly in settings wherein the HSC dose is limiting, such as human CB transplantation (Laughlin et al., 2004; Rocha et al., 2004).

Deletion of Protein Tyrosine Phosphatase Receptor zeta Expands the HSC Pool In Vivo

In the nervous system, PTN can mediate proliferative signals via binding and inhibition of the transmembrane receptor PTPRZ (Meng et al., 2000; Raulo et al., 1994; Stoica et al., 2001). We sought to determine whether PTN mediates HSC self-renewal via inactivation of PTPRZ signaling in HSCs. To that end, we examined the hematopoietic phenotype of Ptprz1$^{-/-}$ mice compared with Ptprz1$^{+/+}$ mice. RT-PCR confirmed the deletion of the full-length messenger RNA transcript for *ptprz* in the

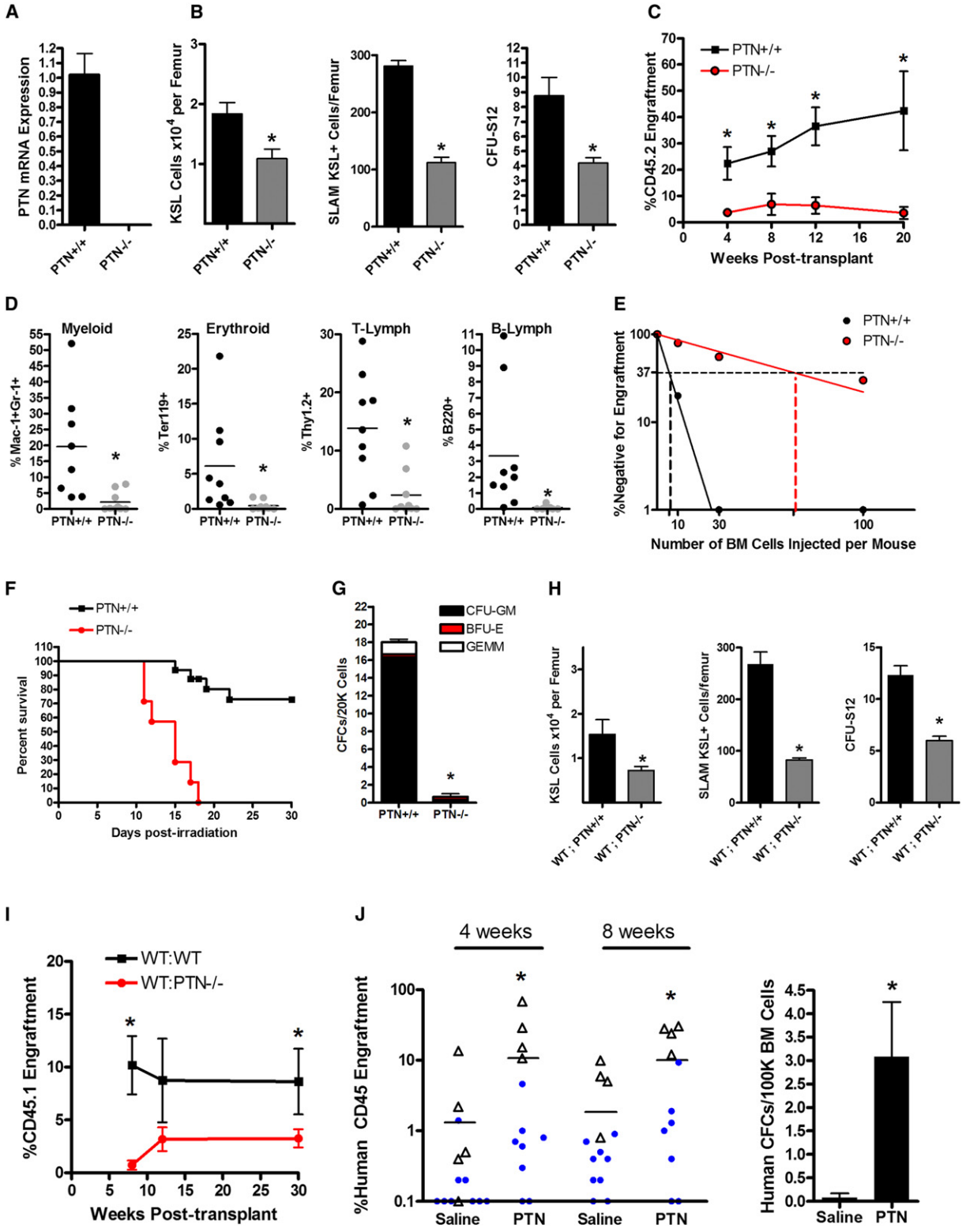

Figure 1. PTN Regulates HSC Self-Renewal and Is Necessary for Hematopoietic Regeneration In Vivo

(A) Quantitative RT-PCR (qRT-PCR) of *ptn* expression in the BM of PTN$^{-/-}$ mice and PTN$^{+/+}$ mice.

(B) PTN$^{-/-}$ mice contained significantly decreased BM KSL cells/femur, SLAM^{+}KSL (CD150^{+}CD48^{-}CD41^{-}lin^{-}c-kit^{+}sca-1^{+}) cells/femur, and BM CFU-S12 compared with PTN$^{+/+}$ mice (n = 4 for KSL, n = 3 for SLAM^{+}KSL, n = 5 for CFU-S12; *p = 0.01, *p = 0.0002, *p = 0.003 respectively).

mutant mice (Figure 2A). Interestingly, 8-week-old Ptprz1$^{-/-}$ mice demonstrated significantly increased white blood cell (WBC), hemoglobin (Hgb), and platelet counts compared with age-matched Ptprz1$^{+/+}$ mice (Figure 2B). Ptprz1$^{-/-}$ mice also displayed significantly increased total BM cells, KSL progenitor cells, CFU-S12, and SLAM^{+}KSL HSCs compared with Ptprz1$^{+/+}$ mice (Figures 2C and 2D). CRU assays demonstrated that mice transplanted with BM 34^{-}KSL cells from Ptprz1$^{-/-}$ mice had 6-fold increased donor CD45.2^{+} cell engraftment at 12 weeks posttransplant compared with mice transplanted with BM cells from Ptprz1$^{+/+}$ mice (Figure 2E). Mice transplanted with HSCs from Ptprz1$^{-/-}$ mice also displayed normal and increased multilineage donor myeloid cell, erythroid cell, T cell, and B cell repopulation compared with recipients of BM from Ptprz1$^{+/+}$ mice, confirming that deletion of PTPRZ did not alter the normal differentiation capacity of BM HSCs (Figure 2F). Mice transplanted with BM cells from Ptprz1$^{-/-}$ mice also demonstrated 5-fold and 10-fold increased donor CD45.2^{+} cell engraftment at 4 weeks and 16 weeks posttransplant, respectively, compared with mice transplanted with BM cells from Ptprz1$^{+/+}$ mice, confirming that deletion of PTPRZ increased both ST- and LT-HSC content in vivo (Figure 2E). A Poisson statistical analysis of donor cell engraftment at 12 weeks from a limiting dilution assay demonstrated a CRU frequency of 1 in 23 in Ptprz1$^{-/-}$ mice (CI: 1/13–1/42) compared with 1 in 72 in Ptprz1$^{+/+}$ mice (CI: 1/27–1/189; Figure 2G). Therefore, deletion of PTPRZ was sufficient to expand the BM HSC pool in vivo, and implicated PTPRZ as the receptor that mediates PTN signaling in HSCs. As evidence that PTPRZ is necessary for PTN-mediated expansion of HSCs, we found that PTN treatment of BM KSL cells from PTPRZ$^{+/+}$ mice caused a significant expansion of KSL cells in vitro, whereas PTN treatment of BM KSL cells from PTPRZ$^{-/-}$ mice failed to expand KSL cells in culture (Figure S2). Of note, we followed Ptprz1$^{-/-}$ mice through 12 months of age and these mice displayed no evidence of splenomegaly, lymphadenopathy, leukemia, or decreased survival compared with Ptprz1$^{+/+}$ mice. These data suggest that deletion of PTPRZ alone does not confer clonal myeloproliferative or lymphoproliferative disease in mice (Figure S3).

PTPRZ Signaling Is HSC Autonomous

To determine whether PTN signaling through PTPRZ is HSC autonomous or mediated via indirect effects on other BM cell types, we transplanted lethally irradiated Bl6.SJL mice (CD45.1^{+}) with BM cells from Ptprz1$^{-/-}$ or Ptprz1$^{+/+}$ mice (CD45.2^{+}) to create Ptprz1$^{-/-}$;WT mice and Ptprz1$^{+/+}$;WT mice. At 8 weeks posttransplant, the recipient mice were $\geq$95% CD45.2^{+}, confirming full donor chimerism (Figure 2H). At this time point, we examined the BM stem/progenitor cell content in both groups of mice. Ptprz1$^{-/-}$;WT mice demonstrated significant increases in BM KSL cells, CFU-S12, and SLAM^{+}KSL HSCs compared with Ptprz1$^{+/+}$;WT mice (Figure 2I). These results demonstrate that PTPRZ-mediated regulation of the HSC pool was HSC autonomous and independent of PTPRZ signaling in the BM microenvironment.

BM ECs and CXCL12^{+} Reticular Cells Express PTN in the HSC Niche

Our transplant studies suggest that maintenance of the HSC pool is dependent upon production of PTN by the BM microenvironment. We next sought to determine which cells within the BM microenvironment produce PTN. Immunostaining of adult mice femurs from PTN green fluorescent protein (PTN-GFP) mice revealed that a subset of VE-cadherin^{+} BM ECs coexpressed PTN, as did vascular endothelial growth factor receptor (VEGFR)3^{+} sinusoidal ECs (Figures 3A and 3B; Butler et al., 2010; Hooper et al., 2009; Salter et al., 2009). Similarly, a subset of CXCL12 (SDF-1)$^{+}$ cells, which appeared to be perivascular,

(C) CD45.1^{+} mice transplanted competitively with a limiting dose (30 cells) of BM CD34^{-}KSL cells from CD45.2^{+} PTN$^{-/-}$ mice demonstrated significantly decreased donor CD45.2^{+} cell engraftment over time compared with mice transplanted with the identical dose of BM CD34^{-}KSL cells from PTN$^{+/+}$ mice (n = 6–10 mice/group; 4 weeks, *p = 0.007; 8 weeks, *p = 0.006; 12 weeks, *p = 0.0008; 20 weeks, *p = 0.02).

(D) Twelve-week myeloid cell (Mac-1^{+}), erythroid cell (Ter119^{+}), T cell (Thy 1.2^{+}), and B cell (B220^{+}) engraftment (*p = 0.004, *p = 0.01, *p = 0.002, and *p = 0.02, respectively, for differences between recipients of BM from PTN$^{+/+}$ and PTN$^{-/-}$ mice).

(E) Poisson statistical analysis after limiting dilution transplant assay. Plots were obtained to allow estimation of the CRU frequency in PTN$^{+/+}$ and PTN$^{-/-}$ mice (n = 9–10 mice transplanted at each cell dose per condition). The plot shows the percentage of recipient (CD45.1^{+}) mice containing <1% CD45.2^{+} cells (nonengrafted) in the PB at 12 weeks posttransplantation (*y* axis) versus the number of cells injected per mouse (*x* axis). The horizontal line indicates the point at which 37% of the mice are nonengrafted, and the vertical lines highlight the CRU frequencies in each mouse (PTN$^{-/-}$ mice [1/66] versus PTN$^{+/+}$ mice [1/6]).

(F) PTN$^{-/-}$ mice displayed increased radiosensitivity compared with PTN$^{+/+}$ mice and failed to regenerate hematopoiesis following TBI. Sixty-nine percent of the PTN$^{+/+}$ mice (11 of 16) were alive at day +30 following 700 cGy TBI (at left). Conversely, none of the PTN$^{-/-}$ mice (0 of 7) survived beyond day +18 ($p < 0.0001$, log rank analysis).

(G) PTN$^{-/-}$ mice had >15-fold decreased BM CFCs at day +20 following TBI compared with PTN$^{+/+}$ mice (at right, n = 3/group, *p = 0.01).

(H) WT;PTN$^{-/-}$ mice had decreased BM KSL cells, decreased SLAM^{+}KSL HSCs, and decreased CFU-S12 compared with WT;PTN$^{+/+}$ mice (means ± SEM, n = 8–9 for KSL and CFU-S12; n = 3 for SLAM analysis; KSL, *p = 0.02; SLAM^{+}KSL, *p = 0.02; CFU-S12, *p = 0.002).

(I) Mice competitively transplanted with a limiting dose (30 cells) of BM CD34^{-}KSL cells from WT;PTN$^{-/-}$ mice demonstrated significantly lower donor CD45.1^{+} cell engraftment over 4–30 weeks compared with mice transplanted with the identical dose of CD34^{-}KSL cells from WT;PTN$^{+/+}$ mice (n = 8 mice/group; 8 weeks, *p = 0.001; 30 weeks, *p = 0.04). Error bars represent SEM for all experiments; Student's t test was performed for comparisons.

(J) NSG mice were irradiated with 250 cGy and then transplanted with human CB mononuclear cells (5–10 × 10^{5} cells/mouse; experiment 1 is represented by blue circles, and experiment 2 is represented by open triangles) followed by intraperitoneal injections of 2 or 4 μg PTN or saline on days +7, +10, and +13 posttransplant. PTN-treated mice displayed significantly increased human hematopoietic cell engraftment in the PB over time posttransplant compared with saline-treated controls (left: n = 11–14 per group, 4 weeks *p = 0.04; 8 weeks *p = 0.03). Horizontal bars represent the mean levels of donor human CD45^{+} cell engraftment. Transplanted NSG mice that were treated with PTN demonstrated significantly increased human CFCs in the BM at 8 weeks compared with saline-treated NSG mice (right: n = 4 mice/group, *p = 0.02).

See also Figure S1.

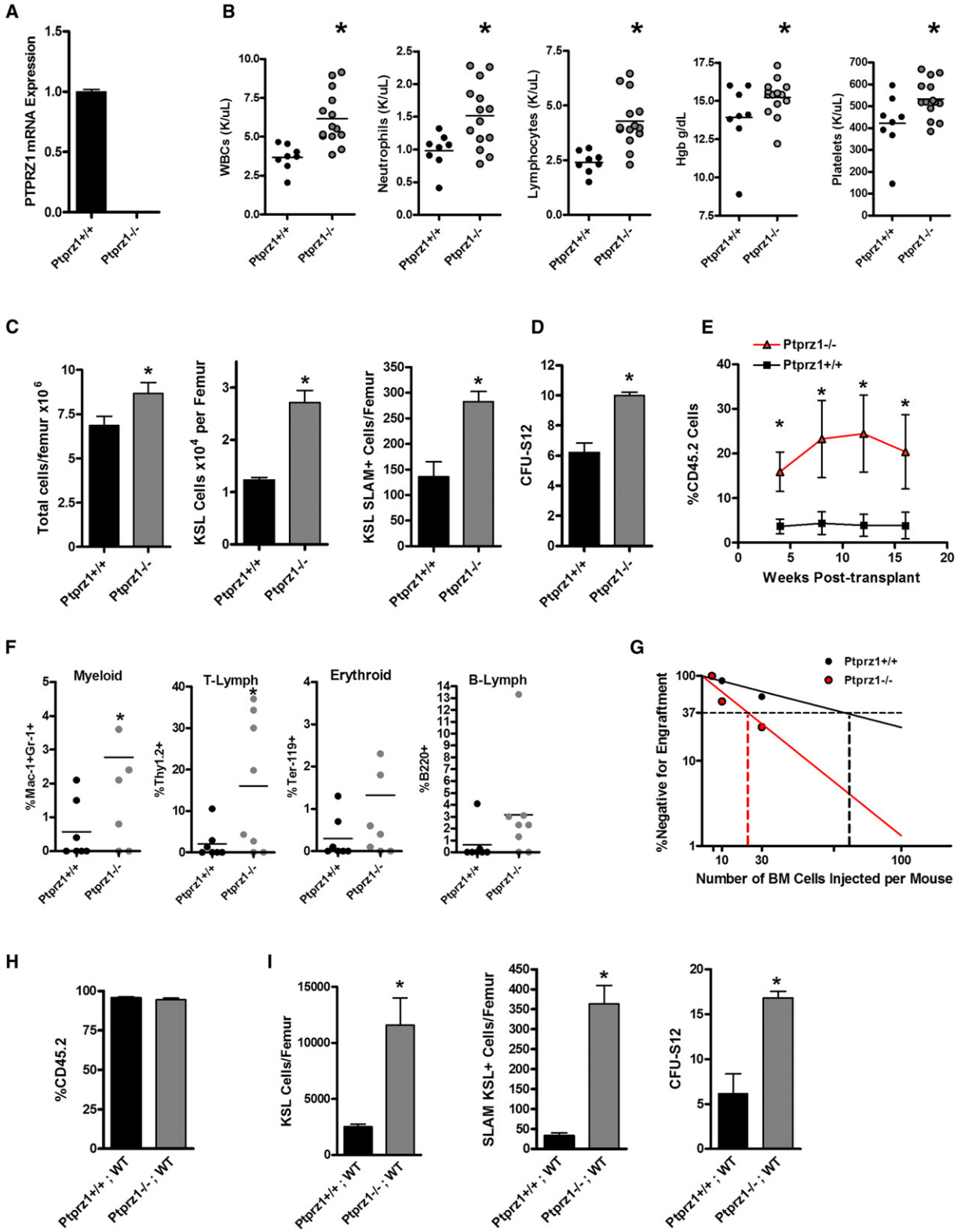

Figure 2. Deletion of PTPRZ Is Sufficient to Expand the BM HSC Pool

(A) qRT-PCR analysis of *ptprz* expression in Ptprz1$^{+/+}$ and Ptprz1$^{-/-}$ mice.

(B) Scatter plots show the complete blood counts in the PB of Ptprz1$^{+/+}$ mice compared with Ptprz1$^{-/-}$ mice (WBCs,*p = 0.005; neutrophils, *p = 0.006; lymphocytes, *p = 0.003; Hgb, *p = 0.04; platelets, *p = 0.01). Mean values are represented by horizontal lines; n = 8–13 mice per condition.

also coexpressed PTN, whereas the majority of osterix$^+$ cells did not express PTN (Figures 3C–3E; Tang et al., 2011). Taken together, these results demonstrate a differential expression of PTN by BM ECs and perhaps by CXCL12-abundant reticular cells (CARs; Sugiyama et al., 2006). We further determined by ELISA that PTN was concentrated within the BM serum of C57Bl6 mice but was not detectable in PB serum (Figure S4). In addition, PTN was highly enriched in the conditioned media from primary BM ECs from C57Bl6 mice, confirming that BM ECs secrete PTN (Figure S4). These results show that PTN is differentially expressed and secreted by principal components of the BM vascular niche and is a paracrine factor for BM stem/progenitor cells in vivo.

To further characterize the cells within the BM niche that expressed PTN, we performed fluorescence-activated cell-sorting (FACS) analysis on BM CD45$^-$PTN$^+$ cells and analyzed for surface expression of the EC marker VE-cadherin. The FACS analysis revealed a distinct population of VE-cadherin$^+$PTN$^+$ cells in the BM (Figure 3F). We then performed a gene expression analysis of FACS-sorted VE-cadherin$^+$PTN$^+$ cells, which revealed enrichment for VEGFR2 and VEGFR3, which are markers of BM sinusoidal endothelium (Hooper et al., 2009; Table 1). Interestingly, VE-cadherin$^+$PTN$^+$ cells were also enriched for expression of CXCL12 and the leptin receptor (lepR), proteins that have been shown to be expressed by both perivascular stromal cells and sinusoidal ECs (Dar et al., 2005; Ding et al., 2012; Ikejima et al., 2004; Sugiyama et al., 2006). VE-cadherin$^+$PTN$^+$ cells lacked expression of Nestin, a marker of BM mesenchymal stromal cells (MSCs) (Méndez-Ferrer et al., 2010).

Lastly, to determine the anatomic relationship between PTN$^+$ cells and HSCs in the BM, we immunostained femurs from PTN-GFP mice to detect CD150$^+$CD48$^-$CD41$^-$lineage$^-$ cells. As previously described, we found CD150$^+$CD48$^-$CD41$^-$lineage$^-$ cells to be rare in the BM (Kiel et al., 2005; Méndez-Ferrer et al., 2010). However, the majority of the CD150$^+$CD48$^-$CD41$^-$lineage$^-$ cells (82.3%, 51 of 62) were found to be in contact with or closely adjacent to PTN$^+$ cells (30 images, 5 femur sections; Figure 3G). Taken together with our functional studies of PTN$^{-/-}$ mice, these results suggest an anatomic and functional relationship between BM HSCs and PTN$^+$ cells in the vascular niche.

PTN Regulates HPC Homing to the BM Niche

Having shown that PTN is expressed by sinusoidal BM ECs within the vascular niche, we sought to determine whether PTN$^+$ ECs regulate HSPC homing to the niche. Adult C57Bl6 mice were injected intravenously with either 50 μg of a specific, neutralizing anti-PTN antibody (R&D Systems) or 50 μg immunoglobulin G (IgG), and after 30 min were infused with 2 × 10^5 BM Sca-1$^+$lin$^-$ progenitor cells from ubiquitin C-GFP (UBC-GFP) mice. At 18 hr posttransplant, the mice were sacrificed and BM cells were analyzed by FACS to compare the homing of GFP$^+$ cells to the BM in each group. Mice that were pretreated with anti-PTN antibody displayed a significant decrease in donor HSPC homing to the BM compared with IgG-treated recipient mice (Figures 4A and 4B). These results suggested that PTN is required for the proper homing of HSPCs to the BM following transplantation. To determine the specific effect that anti-PTN administration had on the homing of transplanted HPCs, we performed intravital imaging using confocal microscopy to observe intravenously transplanted BM lin$^-$GFP$^+$ cells homing within the calvarial BM endothelium in dsRed mice, as previously described (Lo Celso et al., 2011). Mice that were pretreated with IgG and then intravenously transplanted with 3 × 10^6 BM lin$^-$GFP$^+$ cells demonstrated dynamic transmigration of GFP$^+$ cells from the BM vascular space into the BM parenchymal space between 1 and 4 hr posttransplant (Figures 4C and 4D). In contrast, mice that were pretreated with anti-PTN and then transplanted with equal doses of BM lin$^-$GFP$^+$ cells demonstrated a substantial defect in lodgment along the BM endothelium and in transmigration across the BM vasculature into the HSC niche (Figures 4C and 4D). Coupled with the demonstration that anti-PTN quantitatively decreased HSPC homing to the niche, these data suggested an important role for PTN in regulating the lodgment and/or transmigration of HSPCs from the BM vasculature into the HSC niche. Of note, to confirm that systemically administered anti-PTN mediated effects directly upon the BM vascular endothelium, we also show that mice injected with 50 μg anti-PTN-DyLight650 antibody displayed specific binding of the antibody to the intimal endothelial layer of the BM vasculature, whereas mice injected with 50 μg IgG-DyLight650 showed no binding to BM ECs (Figure 4E).

(C) Ptprz1$^{-/-}$ mice have increased mean BM cell counts, KSL cells/femur, and SLAM$^+$KSL cells/femur compared with Ptprz1$^{+/+}$ mice (n = 3–5 mice/group; *p = 0.04, *p = 0.003, *p = 0.002, respectively). Error bars represent SEM.
(D) Ptprz1$^{-/-}$ mice contain increased BM CFU-S12 compared with Ptprz1$^{+/+}$ mice (n = 7–9/group, p < 0.0001).
(E) Mice transplanted with a limiting dose (30 cells) of BM CD34$^-$KSL cells from Ptprz1$^{-/-}$ mice demonstrated significantly higher donor CD45.2$^+$ donor cell engraftment over time compared with recipients of the identical dose of CD34$^-$KSL cells from Ptprz1$^{+/+}$ mice (means ± SEM are shown, n = 7–10 mice/group; 4 weeks, *p = 0.01; 8 weeks, *p = 0.03; 12 weeks, *p = 0.03; 16 weeks, *p = 0.04; Student's t test for all comparisons).
(F) Multilineage engraftment of myeloid cells, erythroid cells, T cells, and B cells is shown at 12 weeks posttransplantation; n = 7–8 mice/group; myeloid, *p = 0.03; T cell, *p = 0.02.
(G) Poisson statistical analysis after limiting dilution transplant assay; plots were obtained to allow estimation of CRU frequency in Ptprz1$^{+/+}$ mice (1 in 72) and Ptprz1$^{-/-}$ mice (1 in 23); n = 7–8 mice transplanted at each cell dose per condition.
(H) The mean percent donor chimerism is shown at 8 weeks posttransplantation of BM cells from Ptprz1$^{+/+}$ or Ptprz1$^{-/-}$ (CD45.2$^+$) mice into lethally irradiated Bl6.SJL recipient (CD45.1$^+$) mice (WT) to generate chimeric Ptprz1$^{-/-}$;WT mice and Ptprz1$^{+/+}$;WT mice. Mean donor cell chimerism was ≥ 95% in Ptprz1$^{-/-}$;WT mice and Ptprz1$^{+/+}$;WT mice (n = 4–5 mice/group, means ± SEM).
(I) Ptprz1$^{-/-}$;WT mice contained significantly increased BM KSL cells/femur, SLAM$^+$KSL cells/femur and CFU-S12 compared with Ptprz1$^{+/+}$;WT mice (n = 3–6/group, *p = 0.004, *p < 0.0001, and *p = 0.002, respectively; data represent means ± SEM; Student's t test for comparisons).
See also Figures S2 and S3.

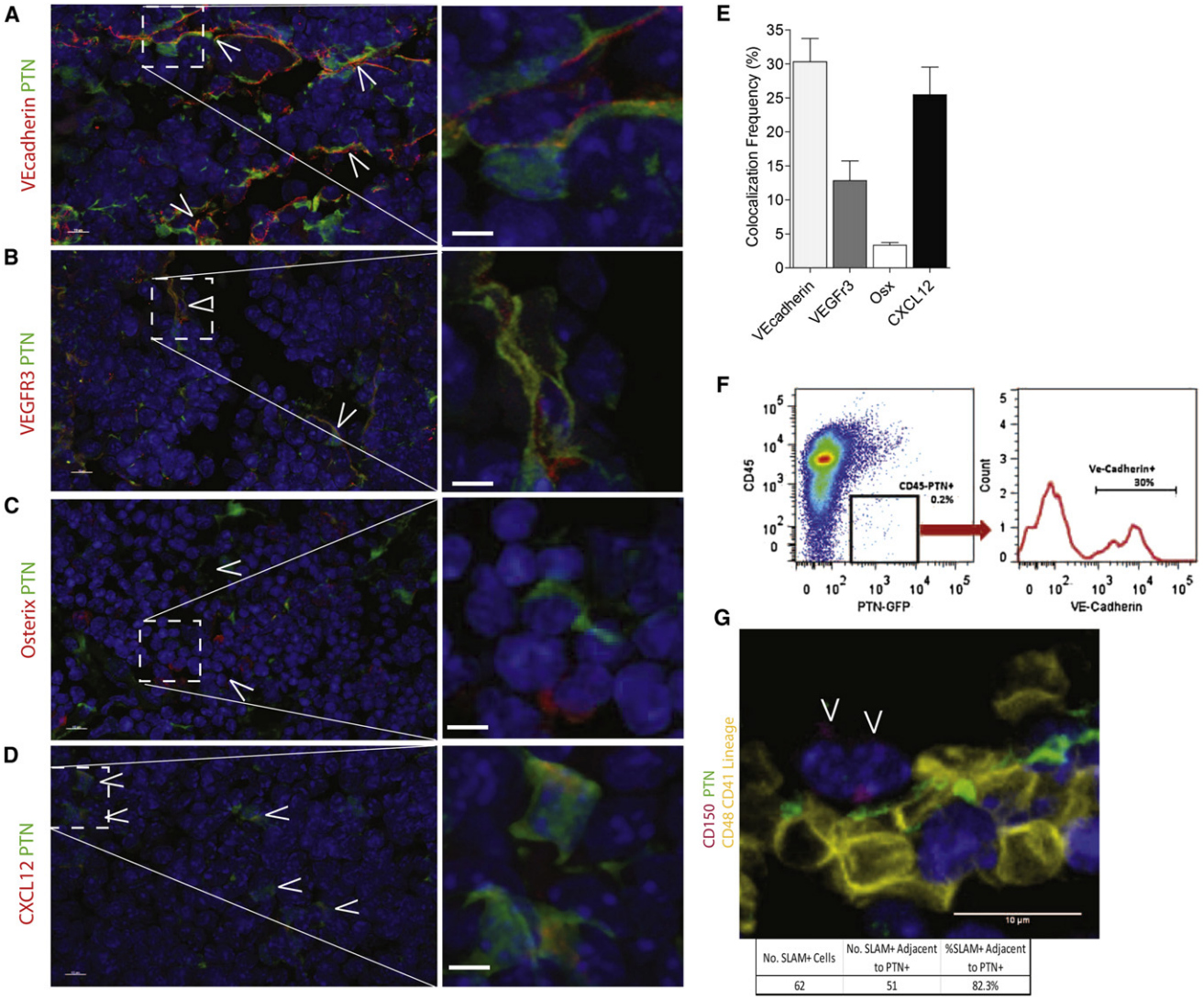

Figure 3. PTN Is Expressed by BM ECs in the HSC Niche

(A) PTN-GFP reporter mice stained with VE-cadherin antibody (red) demonstrate that VE-cadherin$^+$ ECs express PTN (green). White arrows indicate cells that express both PTN and VE-cadherin. Inset box is shown magnified on the right; white scale bar represents 10 μm.

(B) VEGFR3$^+$ sinusoidal vessels (red) that coexpress PTN (green). White arrows indicate cells expressing both VEGFR3 and PTN. Right: High-power image.

(C) Staining for osterix$^+$ cells (red) indicates that very few osterix$^+$ cells express PTN (green). Right: High-power image.

(D) CARs (red) that coexpress PTN (green) are identified. White arrows indicate cells expressing both PTN and CXCL12.

(E) Quantification of the percentage of VE-cadherin$^+$, VEGFR3$^+$, osterix (Osx)$^+$, and CXCL12$^+$ cells that coexpress PTN. Osterix$^+$ cells had the lowest amount of colocalization with PTN-GFP$^+$ cells (3.3%), and 30% of VE-cadherin cells, 12.8% of VEGFR3$^+$ cells, and 25.5% of CXCL12$^+$ cells coexpressed PTN (n = 2–6 tissue sections/stain; bars represent means ± SEM).

(F) Representative FACS analysis of BM cells from PTN-GFP reporter mice costained with CD45 and VE-cadherin antibodies, demonstrating that PTN is expressed by VE-cadherin$^+$ cells.

(G) Immunohistochemical staining for CD150$^+$CD48$^-$CD41$^-$lineage$^-$ cells in the femurs of PTN-GFP mice was performed. A representative image is shown; 82.3% of the CD150$^+$CD48$^-$CD41$^-$lineage$^-$ cells (51 of 62, magenta) were within a 5 μm distance of PTN$^+$ cells (green) in the BM (30 images analyzed from 5 femur sections).

See also Figure S4.

HSPC homing to the BM niche is regulated by numerous cooperative mechanisms, including HSPC rolling, lodgment, and transmigration through BM sinusoidal vasculature, mediated by VLA4–VCAM and CD44–hyaluronic-acid interactions between HSPCs and BM ECs, and via the CXCR4-CXCL12 axis (Avigdor et al., 2004; Kahn et al., 2004; Papayannopoulou et al., 1995). We performed in vitro migration assays in which 2 × 10^5 BM ckit$^+$lin$^-$ cells were placed in the upper chamber of transwell cultures, and 200 ng PTN, 200 ng SDF-1 (CXCL12), or media were placed in the lower chamber. At 4 hr

Table 1. Gene Expression of VE-cadherin$^+$PTN$^+$ Cells

Gene	Description	Fold Difference VE-cad$^+$PTN$^+$	p Value
VEGFR2	Vascular endothelial growth factor receptor 2	84.7	0.006
VEGFR3	Vascular endothelial growth factor receptor 3	68.1	0.02
CXCL12	Chemokine CXC ligand 12	48.0	0.003
LepR	Leptin receptor	136.2	0.02
Nestin	Nestin	ND	

BM cells were collected from PTN-GFP reporter mice and stained with anti-VE-cadherin or isotype antibody. FACS was performed to collect VE-cad$^+$PTN$^+$ cells, and RNA was isolated for qRT-PCR analysis for the genes identified on the left. The fold differences in gene expression between VE-cad$^+$PTN$^+$ cells versus CD45$^+$PTN$^-$ BM cells are shown. n = 3 replicates/group; t test; ND, not detected.

of culture, we observed no migration of HSPCs toward PTN, whereas 35% of HSPCs migrated toward SDF1 (Figure 4F). These data suggested that PTN alone did not provide a gradient for HSPC migration. When HSPCs were preincubated for 1 hr with PTN, we observed a significant increase in HSPC migration toward SDF1, suggesting that PTN augments HSPC migration toward an SDF1 gradient (Figure 4F). However, incubation with PTN did not upregulate CXCR4 or VLA4 expression on BM ckit$^+$lin$^-$ cells, suggesting that PTN regulates HSPC homing through an alternative mechanism (Figure 4F).

Administration of Anti-PTN Promotes HSPC Mobilization

Our results suggest that PTN has an important role in regulating HSPC homing to the BM niche. We further hypothesized that PTN might also regulate HSC retention in the niche, and that systemic administration of anti-PTN might promote HSPC mobilization. To test this hypothesis, we treated adult C57Bl6 mice with either 50 μg IgG, 50 μg anti-PTN, or the CXCR4 antagonist AMD3100 (50 μg) or AMD3100 + anti-PTN. At 1 hr posttreatment, PB was collected and analyzed for mobilization of ckit$^+$sca-1$^+$lin$^-$ cells (KSL cells), which are enriched for HSPCs. Interestingly, treatment with anti-PTN alone significantly increased the number of KSL cells in the PB at 1 hr posttreatment compared with IgG-treated control mice (Figures 4G and 4H). As expected, AMD3100, which is used clinically to mobilize HSPCs (Malard et al., 2012), also promoted HSPC mobilization. Importantly, the combination of AMD3100 and anti-PTN caused a 2-fold increase the mobilization of BM KSL cells compared with the effect of AMD3100 treatment alone (Figures 4G and 4H). Taken together, these data suggest that PTN also regulates the retention of HSPCs in the BM niche and cooperates with the CXCR4-SDF1 axis in this regard.

DISCUSSION

Recent studies have implicated several different cell types within the BM microenvironment as having important roles in regulating HSC self-renewal and retention in vivo (Butler et al., 2010; Calvi et al., 2003; Ding et al., 2012; Hooper et al., 2009; Kiel et al., 2005; Méndez-Ferrer et al., 2010; Salter et al., 2009; Zhang et al., 2003). However, the mechanisms through which BM-microenvironment cells regulate HSC functions in vivo remain incompletely understood. Here we show that PTN, a heparin-binding growth factor, is expressed by sinusoidal ECs within the BM vascular niche and regulates the maintenance of the HSC pool in vivo. Furthermore, genetic deletion of PTPRZ, a receptor for PTN that is expressed by HSCs, caused a significant expansion of the HSC pool in vivo. This observed effect is consistent with the established function of PTN as inactivating PTPZ phosphatase activity upon receptor binding. The observed deficit in HSC numbers coupled with only slight reductions in PB complete blood counts in PTN$^{-/-}$ mice suggests the possibility of compensation by other factors (Herradon et al., 2005) in PTN$^{-/-}$ mice. However, PTN appears to be indispensable for hematopoietic regeneration to occur following myelosuppression, since PTN$^{-/-}$ mice had significantly increased mortality following a myelosuppressive dose of TBI (700 cGy), coupled with a severe deficit in the recovery of BM progenitor cells compared with PTN $^{+/+}$ mice. These results suggest an essential role for PTN in regulating hematopoietic regeneration following injury.

Previous studies identified cellular components of a BM vascular niche for HSCs, including VEGFR2$^+$VEGFR3$^+$ sinusoidal ECs, CARs, and lepR$^+$ perivascular cells, that are essential for maintenance of the HSC pool during homeostasis (Ding et al., 2012; Hooper et al., 2009; Sugiyama et al., 2006). Nestin$^+$ MSCs were also shown to contribute to both the vascular and endosteal niches for HSCs in vivo (Méndez-Ferrer et al., 2010). However, the signaling mechanisms through which cells within the BM vascular niche regulate HSC homeostasis or regeneration are not well understood. Here we demonstrate via immunohistochemical and FACS analyses that PTN is expressed uniquely by VE-cadherin$^+$ ECs that coexpress VEGFR2 and VEGFR3$^+$, consistent with BM sinusoidal ECs (Hooper et al., 2009). Interestingly, PTN$^+$ ECs also express CXCL12 and lepR, which can be expressed by both sinusoidal ECs and perivascular reticular cells (Dar et al., 2005; Ding et al., 2012; Ikejima et al., 2004; Sugiyama et al., 2006). Of note, a prior study (Tezuka et al., 1990) suggested that calvarial bone osteoblasts express PTN, but we found little evidence that osterix$^+$ bone lineage cells expressed PTN in the BM. Commensurate with our findings that PTN was highly expressed by BM sinusoidal ECs, PTN was highly concentrated in BM supernatants and in the conditioned media of primary BM sinusoidal ECs in culture, but was undetectable in the PB of WT mice. These results, coupled with the observed deficit in HSC repopulating cell content in WT;PTN$^{-/-}$ mice, suggest that PTN is an important paracrine factor for HSCs within the vascular niche.

In addition to their role in regulating the maintenance of the HSC pool in vivo, BM sinusoidal ECs regulate the rolling, lodgment, and transmigration of transplanted HSPCs from the vascular space into HSC niches (Avigdor et al., 2004; Papayannopoulou et al., 1995). For example, VLA4–VCAM1 and CD44–hyaluronic-acid interactions between HSPCs and BM ECs control the initial steps in the homing of HSPCs across the vascular endothelium (Avigdor et al., 2004; Papayannopoulou et al., 1995). Because PTN is strongly expressed by BM

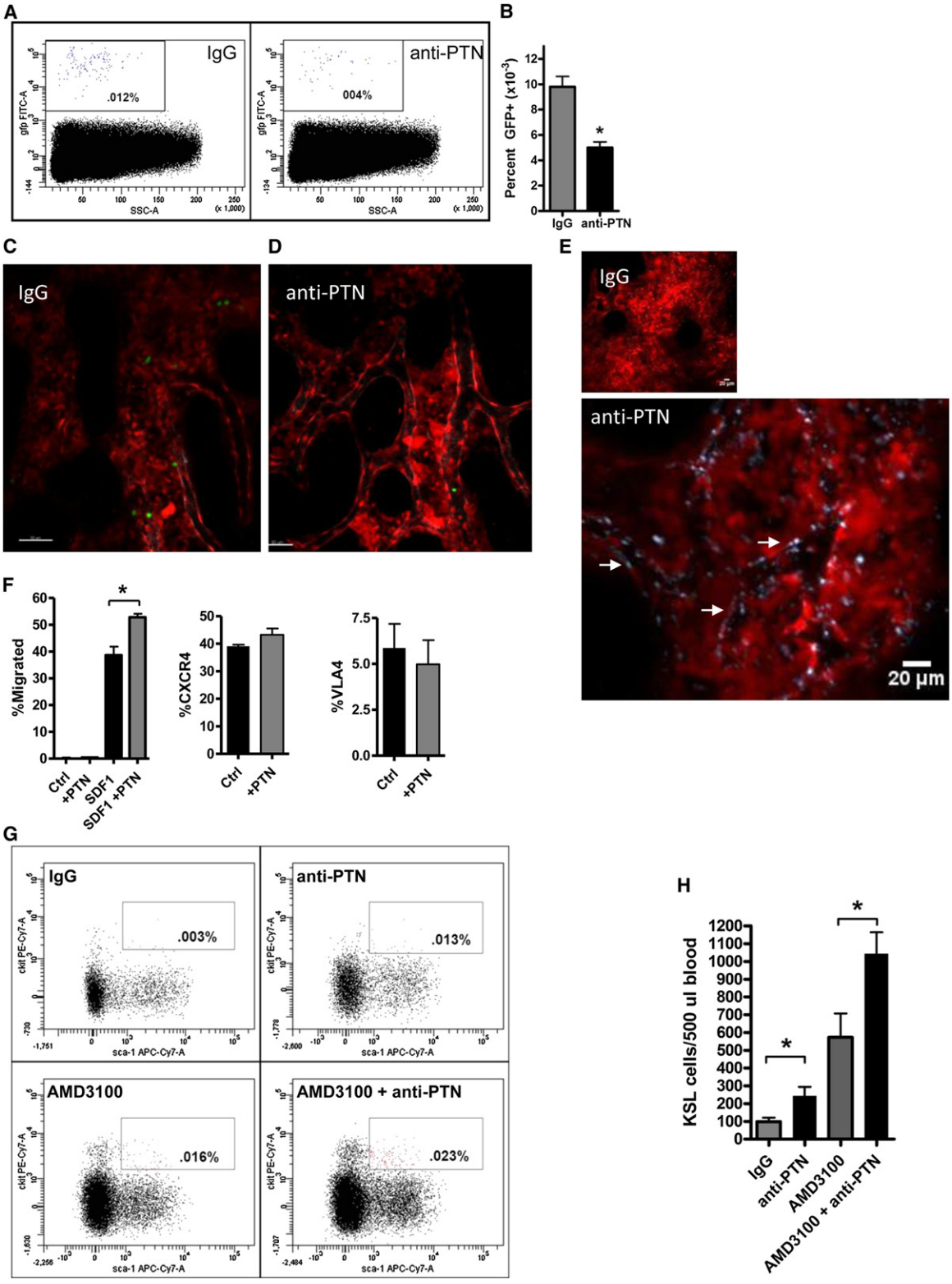

Figure 4. PTN Regulates the Homing and Retention of BM HSPCs

(A) Systemic administration of anti-PTN significantly decreased HSPC homing to the BM niche. Shown is a representative FACS analysis of the percentage GFP$^+$ donor hematopoietic cells in the BM of recipient C57Bl6 mice at 18 hr following intravenous infusion of BM Sca-1$^+$lin$^-$GFP$^+$ cells after pretreatment of recipient mice with either anti-PTN or IgG.

sinusoidal ECs, we sought to determine whether PTN also regulates HSPC migration and homing to the niche. Interestingly, administration of a single dose of anti-PTN antibody substantially inhibited HSPC homing to the niche. Furthermore, intravital imaging revealed that transplanted HSPCs displayed impaired lodgment along the BM endothelium and deficient transmigration from the vascular space into the HSC niche. These data suggest that HSPC anchoring to PTN on sinusoidal ECs may be a critical step in HSPC homing to the BM. In vitro migration assays revealed that HSPCs did not migrate toward a PTN gradient, but pretreatment with PTN did augment HSPC migration toward SDF1. Since PTN treatment did not upregulate CXCR4 or VLA4 expression on HSPCs, PTN may facilitate HSPC homing toward SDF1 via an as yet unidentified mechanism.

In addition to its evident role in regulating the homing of HSPCs to the BM, PTN also regulates the retention of HSPCs in the niche. Administration of a single dose of anti-PTN caused a 2-fold increase in PB HSPCs at 1 hr post-exposure compared with isotype-treated mice, and a similar increase in HSPC mobilization was observed when anti-PTN was combined with AMD3100, a CXCR4 antagonist that is used in clinical practice to mobilize human HSPCs. The rapidity of the effect of anti-PTN administration on HSPC mobilization suggests that PTN plays an important role in the retention of HSPCs in the niche. Moreover, the doubling of HSPC mobilization when anti-PTN was combined with AMD3100 suggests an additive or synergistic role for PTN in modulating HSPC retention via the CXCR4-SDF1 axis. These results also suggest an important potential clinical application for anti-PTN in mobilizing HSPCs in patients undergoing stem cell transplantation.

Istvanffy et al. (2011) recently reported that deletion of PTN in the BM microenvironment was associated with a gain of LT-HSC function compared with mice that retained PTN in the marrow. Important differences between the mouse models used in that study and the one presented here may explain the apparently divergent results: First, we used PTN$^{-/-}$ mice (C57Bl6 background; Jackson Laboratory) and syngeneic (B6.SJL) recipient mice for CRU transplantation studies and for the generation of WT;PTN$^{-/-}$ mice to assess effects of PTN on HSC content. Because these donor and recipient mice were genetically identical, there were no immunological factors that could confound estimates of HSC content. Conversely, in the study by Istvanffy et al. (2011), the CRU assays did not involve syngeneic mice, but rather allogeneic mice. Therefore, immunologic processes such as graft rejection and graft-versus-host reaction, or the effects of PTN on these immune processes, could have affected estimates of HSC content in that model independently of any direct effects of PTN on the HSC pool. Secondly, in this study we used purified HSCs (CD34^{-}KSL cells) for competitive transplantation assays to allow precise determination of the effects of PTN deletion on HSC content and function, whereas Istvanffy et al. (2011) used whole BM cells, and thus it is possible that effects on adventitious cells in the graft could have affected their HSC estimates.

Much remains unknown regarding the mechanisms through which BM-microenvironment cells regulate HSC functions in vivo. Here, we provide evidence that BM sinusoidal ECs uniquely express a secreted protein, PTN, that regulates the maintenance, regeneration, and retention of HSCs in the vascular niche. PTN represents a unique target for pharmacologic approaches to modulate HSC function in vivo.

EXPERIMENTAL PROCEDURES

Mice

All animal procedures were performed in accordance with a Duke University IACUC-approved animal use protocol. Embryos from mice bearing a constitutive deletion of PTN (Ochiai et al., 2004) were obtained from the RIKEN Institute (Tsukuba, Japan) by the Jackson Laboratory (Bar Harbor, ME) and rederived in a C57BL6 background. Mice bearing a constitutive deletion of the PTN

(B) Anti-PTN treated mice had >2-fold decreased donor GFP^{+} cells in the BM at 18 hr postinfusion compared with IgG-treated control mice (n = 5–6/group, means ± SEM, *p = 0.0004).

(C and D) Administration of anti-PTN inhibits the lodgment and transmigration of HPCs from the BM vasculature into the stem cell niche. Representative intravital images of the calvarial BM space in living dsRed mice during the first 4 hr postintravenous infusion of 3 × 10^{6} BM lin^{-}GFP^{+} cells are shown. Mice that were pretreated with IgG antibody (C) demonstrated abundant homing of transplanted cells (green) from the BM sinusoidal vasculature (gray) into the niche, whereas mice pretreated with anti-PTN displayed a markedly decreased number of donor HPCs within the extravascular BM space (D). A single GFP^{+} cell (green) is shown within the BM vasculature in the anti-PTN-treated mice.

(E) Systemically administered anti-PTN binds extensively to the BM sinusoidal vasculature. Shown is a representative intravital image of the calvarial BM of dsRed mice at 30 min after intravenous injection of either IgG-DyLight650 antibody (left: 20×, scale bar 50 μm) or anti-PTN-DyLight650 (middle: 20×, scale bar 50 μm). Binding and illumination of the BM sinusoidal vasculature by anti-PTN antibody (gray outline, white arrows) is shown in high power at right (4× zoom of the white box area in the previous image; scale bar 20 μm).

(F) Preincubation with PTN augments HPC migration to an SDF1 gradient. BM ckit^{+}lin^{-} cells demonstrated no migration to media alone or PTN in a 4 hr transwell assay (left, n = 4/group). A percentage of BM ckit^{+}lin^{-} cells migrated to an SDF1 gradient in the lower chamber of transwell cultures. Left: BM ckit^{+}lin^{-} cells that were preincubated with PTN × 1 hr demonstrated significantly increased migration to SDF1 compared with control cultures at 4 hr in transwell assay (n = 6/group, means ± SEM, *p = 0.002). Incubation of BM ckit^{+}lin^{-} cells with PTN had no effect on cell-surface expression of CXCR4 (middle) or VLA4 (right); n = 6/group, means ± SEM.

(G) Administration of anti-PTN promoted the rapid mobilization of HSPCs in WT mice. Shown are representative FACS plots of the percentage of KSL cells in the PB of adult C57Bl6 mice at 1 hr following intravenous administration of IgG, anti-PTN, AMD3100, or AMD3100 + anti-PTN. Both anti-PTN and AMD3100 increased the mobilization of KSL cells to the PB compared with IgG-treated control mice. Mice treated with AMD3100 + anti-PTN displayed increased KSL cell mobilization compared with AMD3100 treatment alone.

(H) The bar graphs show the means ± SEM of KSL cells in the PB of IgG-treated mice, anti-PTN-treated mice, AMD3100-treated mice, and mice treated with AMD3100 + anti-PTN. Treatment with anti-PTN alone or in combination with AMD3100 significantly increased KSL cell mobilization compared with IgG-treated or AMD3100-treated mice, respectively. *p = 0.02 for anti-PTN versus IgG (n = 8/group, means ± SEM); *p = 0.03 for AMD3100 + anti-PTN versus AMD3100 alone (n = 5/group, means ± SEM).

receptor PTPRZ were a generous gift from Dr. Sheila Harroch of L'Institut Pasteur, Paris, France (Harroch et al., 2000, 2002). Sperm from PTN-GFP mice developed as part of the GENSAT Project (Rockefeller University) was obtained from the Mutant Mouse Regional Resource Center and the strain was rederived in a C57BL6 background.

Isolation of Murine BM HSCs

BM HSCs were collected from all mice as previously described (Himburg et al., 2010). Briefly, collected BM was first treated with red blood cell (RBC)-lysis buffer (Sigma Aldrich), and lineage committed cells were removed using a lineage depletion column (Miltenyi Biotec, Auburn CA). Lin^- cells were stained with fluorescein isothiocyanate-conjugated anti-CD34 (eBioscience, San Diego, CA), PE-conjugated anti-sca-1, and APC-conjugated anti-ckit (Becton Dickinson [BD], San Jose, CA), or isotype controls. Sterile cell sorting was conducted on a BD FACS-Aria cytometer. Purified $CD34^-c\text{-}kit^+sca\text{-}1^+lin^-$ (34^-KSL) subsets were collected into Iscove's modified Dulbecco's medium (IMDM) + 10% fetal bovine serum (FBS) + 1% pcn/strp.

Colony-Forming-Cell and CFU-S12 Assays

Colony-forming-cell (CFC) assays (CFU-granulocyte monocyte [CFU-GM], burst-forming unit-erythroid [BFU-E], and CFU-mix [CFU-GEMM]) were performed in triplicate as previously described (Chute et al., 2002, 2005). Briefly, 5,000 cells from each condition were placed in MethoCult (StemCell Technologies, Vancouver, Canada) for 14 days, and the total colonies were calculated. The BM HSC content in the mutant mice was assayed by CFU-S12 assay. RBC-depleted BM was transplanted at a dose of 1×10^5 cells/mouse into lethally irradiated (950 cGy) C57Bl6 mice. At day 12 post-transplant, the mice were euthanized and the spleens were collected. The numbers of hematopoietic colonies on each spleen were counted.

CRU Assay

BM 34^-KSL cells from the $PTN^{-/-}$ and $Ptprz1^{-/-}$ mice, and $PTN^{+/+}$ and $Ptprz1^{+/+}$ mice carrying the CD45.2 allele were isolated by FACS (Himburg et al., 2010). Recipient B6.SJL animals expressing the CD45.1 allele received 950 cGy TBI via a Cs137 irradiator and were then transplanted via tail vein injection with 5, 10, 30, or 100 BM 34^-KSL cells. Nonirradiated host BM mononuclear cells (MNCs; 1×10^5 cells/mouse) were injected as competitor cells. Multilineage hematologic reconstitution was monitored in the PB by flow cytometry, as previously described (Chute et al., 2007; Himburg et al., 2010), at 4, 8, 12, 16, and 20 weeks posttransplant. PB was collected via submandibular puncture and stained with antilineage marker antibodies as previously described (Himburg et al., 2010). Animals were considered to be engrafted if donor CD45.2 cells were present at $\geq$1%. CRU calculations were performed with the use of L-Calc software (Stem Cell Technologies; Chute et al., 2005, 2006b).

PTN Reporter Mice

PTN-GFP reporter mice (Jackson Laboratory) were given an intravenous injection of 200 μg of rat anti-mouse Alexa Fluor 647 VE-cadherin antibody in PBS. The mice were sacrificed within 1 hr of injection and the BM was flushed through a 30 μm filter in Hanks' balanced salt solution with Ca^{2+} and Mg^{2+}. The portion of the BM retained in the 30 μm filter was collected and mechanically disrupted by pipetting. The filter-retained cells were then stained with PerCP-conjugated CD45 and FACs sorted to obtain $CD45^-VE\text{-}cadherin^+PTN^+$ and $CD45^-VE\text{-}cadherin^-PTN^+$ cells. These populations were compared with the $CD45^+PTN^-$ cell population for RT-PCR analysis.

PTN Treatment of $Ptprz1^{-/-}$ Cells In Vitro

$CD34^-KSL$ cells were isolated from $Ptprz1^{-/-}$ and $Ptprz^{+/+}$ mice and cultured for 7 days in IMDM containing 10% FBS, 1% pen-strep, 125 ng/ml stem cell factor, 50 ng/ml Flt-3 ligand, and 20 ng/ml thrombopoietin either with or without 100 ng/ml PTN. Following culture, the progeny were analyzed for total KSL cell expansion.

Human CB Transplant Model

Human CB units were obtained according to a protocol approved by the Institutional Review Board of Duke University. The units were purified for MNCs using a density gradient separation in Ficoll-HyPaque followed by RBC lysis. Then $0.5–1 \times 10^6$ human CB MNCs were transplanted into 6-week-old NSG mice conditioned with 250 cGy radiation on a Cesium source. Following transplantation, the mice were treated intraperitoneally on days +7, +10, and +13 posttransplant with 2–4 μg PTN or saline. PB was drawn retro-orbitally at 4 and 8 weeks posttransplant to assess human $CD45^+$ cell engraftment.

SUPPLEMENTAL INFORMATION

Supplemental Information includes Extended Experimental Procedures and four figures and can be found with this article online at http://dx.doi.org/10.1016/j.celrep.2012.09.002.

LICENSING INFORMATION

ACKNOWLEDGMENTS

The authors thank Dr. Joel Ross for assistance with graphical art. This work was supported in part by National Institute for Allergy and Infectious Diseases grant AI067798-06 (J.P.C.) and National Heart, Lung and Blood Institute grant HL086998-01 (J.P.C.).

Received: March 25, 2011
Revised: February 10, 2012
Accepted: September 6, 2012
Published online: October 18, 2012

REFERENCES

Avigdor, A., Goichberg, P., Shivtiel, S., Dar, A., Peled, A., Samira, S., Kollet, O., Hershkoviz, R., Alon, R., Hardan, I., et al. (2004). CD44 and hyaluronic acid cooperate with SDF-1 in the trafficking of human CD34+ stem/progenitor cells to bone marrow. Blood *103*, 2981–2989.

Blank, U., Karlsson, G., and Karlsson, S. (2008). Signaling pathways governing stem-cell fate. Blood *111*, 492–503.

Butler, J.M., Nolan, D.J., Vertes, E.L., Varnum-Finney, B., Kobayashi, H., Hooper, A.T., Seandel, M., Shido, K., White, I.A., Kobayashi, M., et al. (2010). Endothelial cells are essential for the self-renewal and repopulation of Notch-dependent hematopoietic stem cells. Cell Stem Cell *6*, 251–264.

Calvi, L.M., Adams, G.B., Weibrecht, K.W., Weber, J.M., Olson, D.P., Knight, M.C., Martin, R.P., Schipani, E., Divieti, P., Bringhurst, F.R., et al. (2003). Osteoblastic cells regulate the haematopoietic stem cell niche. Nature *425*, 841–846.

Chute, J.P., Saini, A.A., Chute, D.J., Wells, M.R., Clark, W.B., Harlan, D.M., Park, J., Stull, M.K., Civin, C., and Davis, T.A. (2002). Ex vivo culture with human brain endothelial cells increases the SCID-repopulating capacity of adult human bone marrow. Blood *100*, 4433–4439.

Chute, J.P., Muramoto, G., Fung, J., and Oxford, C. (2004). Quantitative analysis demonstrates expansion of SCID-repopulating cells and increased engraftment capacity in human cord blood following ex vivo culture with human brain endothelial cells. Stem Cells *22*, 202–215.

Chute, J.P., Muramoto, G.G., Fung, J., and Oxford, C. (2005). Soluble factors elaborated by human brain endothelial cells induce the concomitant expansion of purified human BM CD34+CD38− cells and SCID-repopulating cells. Blood *105*, 576–583.

Chute, J.P., Muramoto, G.G., Dressman, H.K., Wolfe, G., Chao, N.J., and Lin, S. (2006a). Molecular profile and partial functional analysis of novel endothelial cell-derived growth factors that regulate hematopoiesis. Stem Cells *24*, 1315–1327.

Chute, J.P., Muramoto, G.G., Whitesides, J., Colvin, M., Safi, R., Chao, N.J., and McDonnell, D.P. (2006b). Inhibition of aldehyde dehydrogenase and retinoid signaling induces the expansion of human hematopoietic stem cells. Proc. Natl. Acad. Sci. USA *103*, 11707–11712.

Chute, J.P., Muramoto, G.G., Salter, A.B., Meadows, S.K., Rickman, D.W., Chen, B., Himburg, H.A., and Chao, N.J. (2007). Transplantation of vascular endothelial cells mediates the hematopoietic recovery and survival of lethally irradiated mice. Blood *109*, 2365–2372.

Dar, A., Goichberg, P., Shinder, V., Kalinkovich, A., Kollet, O., Netzer, N., Margalit, R., Zsak, M., Nagler, A., Hardan, I., et al. (2005). Chemokine receptor CXCR4-dependent internalization and resecretion of functional chemokine SDF-1 by bone marrow endothelial and stromal cells. Nat. Immunol. *6*, 1038–1046.

Ding, L., Saunders, T.L., Enikolopov, G., and Morrison, S.J. (2012). Endothelial and perivascular cells maintain haematopoietic stem cells. Nature *481*, 457–462.

Harroch, S., Palmeri, M., Rosenbluth, J., Custer, A., Okigaki, M., Shrager, P., Blum, M., Buxbaum, J.D., and Schlessinger, J. (2000). No obvious abnormality in mice deficient in receptor protein tyrosine phosphatase beta. Mol. Cell. Biol. *20*, 7706–7715.

Harroch, S., Furtado, G.C., Brueck, W., Rosenbluth, J., Lafaille, J., Chao, M., Buxbaum, J.D., and Schlessinger, J. (2002). A critical role for the protein tyrosine phosphatase receptor type Z in functional recovery from demyelinating lesions. Nat. Genet. *32*, 411–414.

Herradon, G., Ezquerra, L., Nguyen, T., Silos-Santiago, I., and Deuel, T.F. (2005). Midkine regulates pleiotrophin organ-specific gene expression: evidence for transcriptional regulation and functional redundancy within the pleiotrophin/midkine developmental gene family. Biochem. Biophys. Res. Commun. *333*, 714–721.

Himburg, H.A., Muramoto, G.G., Daher, P., Meadows, S.K., Russell, J.L., Doan, P., Chi, J.T., Salter, A.B., Lento, W.E., Reya, T., et al. (2010). Pleiotrophin regulates the expansion and regeneration of hematopoietic stem cells. Nat. Med. *16*, 475–482.

Hooper, A.T., Butler, J.M., Nolan, D.J., Kranz, A., Iida, K., Kobayashi, M., Kopp, H.G., Shido, K., Petit, I., Yanger, K., et al. (2009). Engraftment and reconstitution of hematopoiesis is dependent on VEGFR2-mediated regeneration of sinusoidal endothelial cells. Cell Stem Cell *4*, 263–274.

Ikejima, K., Lang, T., Zhang, Y.J., Yamashina, S., Honda, H., Yoshikawa, M., Hirose, M., Enomoto, N., Kitamura, T., Takei, Y., and Sato, N. (2004). Expression of leptin receptors in hepatic sinusoidal cells. Comp. Hepatol. *3*(*Suppl 1*), S12.

Istvanffy, R., Kröger, M., Eckl, C., Gitzelmann, S., Vilne, B., Bock, F., Graf, S., Schiemann, M., Keller, U.B., Peschel, C., and Oostendorp, R.A. (2011). Stromal pleiotrophin regulates repopulation behavior of hematopoietic stem cells. Blood *118*, 2712–2722.

Kahn, J., Byk, T., Jansson-Sjostrand, L., Petit, I., Shivtiel, S., Nagler, A., Hardan, I., Deutsch, V., Gazit, Z., Gazit, D., et al. (2004). Overexpression of CXCR4 on human CD34+ progenitors increases their proliferation, migration, and NOD/SCID repopulation. Blood *103*, 2942–2949.

Kiel, M.J., and Morrison, S.J. (2008). Uncertainty in the niches that maintain haematopoietic stem cells. Nat. Rev. Immunol. *8*, 290–301.

Kiel, M.J., Yilmaz, O.H., Iwashita, T., Yilmaz, O.H., Terhorst, C., and Morrison, S.J. (2005). SLAM family receptors distinguish hematopoietic stem and progenitor cells and reveal endothelial niches for stem cells. Cell *121*, 1109–1121.

Laughlin, M.J., Eapen, M., Rubinstein, P., Wagner, J.E., Zhang, M.J., Champlin, R.E., Stevens, C., Barker, J.N., Gale, R.P., Lazarus, H.M., et al. (2004). Outcomes after transplantation of cord blood or bone marrow from unrelated donors in adults with leukemia. N. Engl. J. Med. *351*, 2265–2275.

Li, Y.S., Milner, P.G., Chauhan, A.K., Watson, M.A., Hoffman, R.M., Kodner, C.M., Milbrandt, J., and Deuel, T.F. (1990). Cloning and expression of a developmentally regulated protein that induces mitogenic and neurite outgrowth activity. Science *250*, 1690–1694.

Lo Celso, C., Lin, C.P., and Scadden, D.T. (2011). In vivo imaging of transplanted hematopoietic stem and progenitor cells in mouse calvarium bone marrow. Nat. Protoc. *6*, 1–14.

Malard, F., Kröger, N., Gabriel, I.H., Hübel, K., Apperley, J.F., Basak, G.W., Douglas, K.W., Geraldes, C., Jaksic, O., Koristek, Z., et al. (2012). Plerixafor for autologous peripheral blood stem cell mobilization in patients previously treated with fludarabine or lenalidomide. Biol. Blood Marrow Transplant. *18*, 314–317.

Méndez-Ferrer, S., Michurina, T.V., Ferraro, F., Mazloom, A.R., Macarthur, B.D., Lira, S.A., Scadden, D.T., Ma'ayan, A., Enikolopov, G.N., and Frenette, P.S. (2010). Mesenchymal and haematopoietic stem cells form a unique bone marrow niche. Nature *466*, 829–834.

Meng, K., Rodriguez-Peña, A., Dimitrov, T., Chen, W., Yamin, M., Noda, M., and Deuel, T.F. (2000). Pleiotrophin signals increased tyrosine phosphorylation of beta beta-catenin through inactivation of the intrinsic catalytic activity of the receptor-type protein tyrosine phosphatase beta/zeta. Proc. Natl. Acad. Sci. USA *97*, 2603–2608.

Ochiai, K., Muramatsu, H., Yamamoto, S., Ando, H., and Muramatsu, T. (2004). The role of midkine and pleiotrophin in liver regeneration. Liver Int. *24*, 484–491.

Papayannopoulou, T., Craddock, C., Nakamoto, B., Priestley, G.V., and Wolf, N.S. (1995). The VLA4/VCAM-1 adhesion pathway defines contrasting mechanisms of lodgement of transplanted murine hemopoietic progenitors between bone marrow and spleen. Proc. Natl. Acad. Sci. USA *92*, 9647–9651.

Raulo, E., Chernousov, M.A., Carey, D.J., Nolo, R., and Rauvala, H. (1994). Isolation of a neuronal cell surface receptor of heparin binding growth-associated molecule (HB-GAM). Identification as N-syndecan (syndecan-3). J. Biol. Chem. *269*, 12999–13004.

Rocha, V., Labopin, M., Sanz, G., Arcese, W., Schwerdtfeger, R., Bosi, A., Jacobsen, N., Ruutu, T., de Lima, M., Finke, J., et al; Acute Leukemia Working Party of European Blood and Marrow Transplant Group; Eurocord-Netcord Registry. (2004). Transplants of umbilical-cord blood or bone marrow from unrelated donors in adults with acute leukemia. N. Engl. J. Med. *351*, 2276–2285.

Salter, A.B., Meadows, S.K., Muramoto, G.G., Himburg, H., Doan, P., Daher, P., Russell, L., Chen, B., Chao, N.J., and Chute, J.P. (2009). Endothelial progenitor cell infusion induces hematopoietic stem cell reconstitution in vivo. Blood *113*, 2104–2107.

Stoica, G.E., Kuo, A., Aigner, A., Sunitha, I., Souttou, B., Malerczyk, C., Caughey, D.J., Wen, D., Karavanov, A., Riegel, A.T., and Wellstein, A. (2001). Identification of anaplastic lymphoma kinase as a receptor for the growth factor pleiotrophin. J. Biol. Chem. *276*, 16772–16779.

Sugiyama, T., Kohara, H., Noda, M., and Nagasawa, T. (2006). Maintenance of the hematopoietic stem cell pool by CXCL12-CXCR4 chemokine signaling in bone marrow stromal cell niches. Immunity *25*, 977–988.

Tang, W., Li, Y., Osimiri, L., and Zhang, C. (2011). Osteoblast-specific transcription factor Osterix (Osx) is an upstream regulator of Satb2 during bone formation. J. Biol. Chem. *286*, 32995–33002.

Tezuka, K., Takeshita, S., Hakeda, Y., Kumegawa, M., Kikuno, R., and Hashimoto-Gotoh, T. (1990). Isolation of mouse and human cDNA clones encoding a protein expressed specifically in osteoblasts and brain tissues. Biochem. Biophys. Res. Commun. *173*, 246–251.

Zhang, J., Niu, C., Ye, L., Huang, H., He, X., Tong, W.G., Ross, J., Haug, J., Johnson, T., Feng, J.Q., et al. (2003). Identification of the haematopoietic stem cell niche and control of the niche size. Nature *425*, 836–841.

Zon, L.I. (2008). Intrinsic and extrinsic control of haematopoietic stem-cell self-renewal. Nature *453*, 306–313.